ISBN: 978-3-95450-208-0 doi:10.18429/JACoW-IPAC2019-TUPRB101

DAMPING TRAPPED MODES IN AN IN-VACUUM UNDULATOR AT A SYNCHROTRON RADIATION LIGHT SOURCE*

K. Tian†, A. D. Ringwall, J. J. Sebek, Z. Li
SLAC National Accelerator Laboratory,Menlo Park, CA, USA

Abstract

In this paper, we report the efforts in solving the problem of coupled-bunch instabilities caused by an in-vacuum undulator in the SPEAR3 storage ring. After exploring several approaches to reduce the strength of the trapped modes, we found that ferrite dampers were the most effective and simplest way for mode damping in our SPEAR3 in-vacuum undulator. The results of the first RF cold measurement on an in-vacuum undulator equipped with these ferrite dampers agree well with numerical simulations.

INTRODUCTION

SPEAR3 is a 3 GeV, 500 mA, third generation light source. The 2-meter-long BL15 insertion device (BL15 ID) in SPEAR3 is the second IVU in the storage ring with an undulator period of 22 mm. During early commissioning of the BL15 ID, we observed that the transverse beam size increased at small, discrete magnet gaps with 500 mA stored beam. Similar problems have been reported and investigated in other facilities as well [1–3]. Upon further investigation, we discovered that the beam size increase was caused by transverse coupled-bunch instabilities driven by the trapped resonant modes inside the IVU chamber [4, 5]. The geometry of the IVU chamber, with the magnetic structure, resembles many features of a round ridge waveguide [6–8], which supports lower frequency modes that can be trapped inside the bare vacuum chamber. A transverse mode can be excited by the bunches in the ring. This mode, in turn, if sufficiently strong, can drive the beam unstable. The IVUs are designed for variable gap operations, therefore, the spectrum of the trapped modes shifts in frequency with the changes in the magnet gap of the IVU. The coupling impedance is sufficiently strong that when the mode frequency overlaps the lower vertical betatron sideband of a revolution harmonic [9], vertical instabilities are excited in SPEAR3.

Most modern storage rings, including SPEAR3, are equipped with multi-bunch feedback systems, which have been successfully demonstrated to be effective in damping these, and other, transverse coupled-bunch instabilities [10–12]. However it is preferable to passively eliminate the source of the instability rather than to rely on active damping. In this paper, we will present a passive damping technique using ferrite dampers inside the IVU chamber to damp the trapped modes.

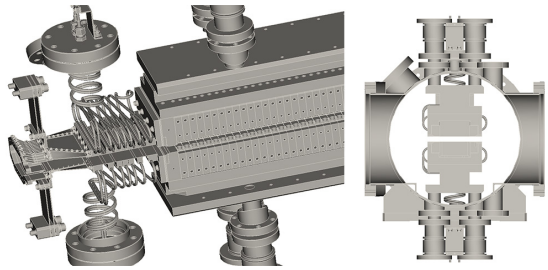

Figure 1: The CAD model for the IVU chamber. Left: the IVU structure inside the chamber with the flexible transition; right: view of the cross section of the IVU device that resembles a round ridge wave guide. (Courtesy of Neomax Engineering Co.)

NUMERICAL SIMULATION

Numerical simulations for studying the HOM modes that cause the beam instabilities have been carried out using a parallel code, Omega3P, running on the super computer, Cori, at the National Energy Research Scientific Computing Center (NERSC) [13]. The simulation model mesh was constructed using CUBIT [14]; the data was visualized using ParaView [15].

The IVU chamber contains numerous components for various purposes. Therefore, it is necessary to build a model that is sufficiently simple to perform numerical simulations, while still good enough for accurately studying the RF properties of the structure. The mode frequency of interest for the IVU chamber is around 200 MHz. Therefore, as a rule of thumb, geometrical features with dimensions less than 10 cm, or 1/15 of the RF wavelength can be considered to be small and generally have less impact on the RF properties of the mode. We started with a highly simplified structure before gradually adding more features and keeping only those that significantly affect the simulation results.

The actual magnet row is 1954 mm long with transitions of lengths greater than 100 mm at each end. As shown in Fig. 1, the top and bottom magnet rows are attached to two I-beam shaped in-vacuum girders made of aluminum. Each of the two in-vacuum girders is connected to the out-of-vacuum mechanical gap motion system through 12 bellows link rods. These rods, which connect the girders and the outside chamber, have significant impacts on field patterns and frequencies of the RF modes. Therefore, we model the magnet row assembly with a 1954 mm long metal bar with a rectangular cross-section measuring about the same size

* Work supported by US Department of Energy Contract DE-AC03-76SF00515. This research used resources of the National Energy Research Scientific Computing Center (NERSC), a U.S. Department of Energy Office of Science User Facility operated under Contract No. DE-AC02-05CH11231.
† email address:ktian@slac.stanford.edu

ISBN: 978-3-95450-208-0 doi:10.18429/JACoW-IPAC2019-TUPRB101

as that of the assembly. To reduce the resistive wall beam impedance and that contributed from the short range wakefields, a nickel-plated copper foil is attached to the permanent magnet (PMs) poles through magnetic attractive force to provide a highly conductive smooth surface on top of the magnet arrays. In addition, a flexible transition based on an SLS design [16] connects the PM gap to the entrance/exit of the vacuum chamber. Due to thermal concerns, the transition is cooled by a complex water cooling system. Because the wavelengths of the modes of interest are much larger than the dimension of the cooling structure, a combination of a brick and a cylinder is used to represent the cooling system. The flexible section provides a smooth transition, but with the variation of the magnet gap, the profile for the transition is varied as well. Therefore, it is hard to model the exact boundary geometry for the electron beam when passing through the transition. Therefore we model the transition by first selecting several points along the transition, which fix the geometry relations to the magnet gap, and then linearly interpolate between them. Finally, after considering the RF impacts of most of the major geometric features in the IVU chamber, we build for numerical studies a model as shown in Fig. 2.

DAMPER DESIGN

Although the IVU chamber supports numerous RF modes, only those at lower frequencies have strong transverse coupling impedances and therefore a strong interaction with the electron beam. A close examination of the electromagnetic fields shows that these modes all belong to the same series of TE type resonant modes, each with a different longitudinal mode number. In the following, we will simply refer to them as the ridge waveguide modes. The first ridge waveguide mode, or HOM #1, is the first harmonic with nodes only at the longitudinal boundaries, giving a half cycle of RF field variation in the longitudinal direction. HOMs #2 and #3, the modes responsible for the coupled-bunch instabilities in BL15 ID, are the second and the third harmonic with a full cycle and one and one-half cycles of field variation in the longitudinal direction, respectively. Both the electric and magnetic fields of a ridge-waveguide mode are concentrated at the narrow magnet gap. Damping of both electric and magnetic fields is electromagnetically possible by placing the appropriate absorptive material in or near the gap. While the electric field in the rest of the chamber remain very small, significant magnet fields leak out of the magnet gap and fill the vast space in the chamber. Therefore, if one is limited by practical considerations to placing damping materials only away from the gap, we are limited to absorptive magnetic material. Especially, the magnetic field is enhanced around the bellows of the linked rods. Therefore these modes can be effectively damped by adding magnetic damping materials around these rods. Furthermore, in order to achieve the full spectrum damping to all the ridge-waveguide modes, it is prudent to add the damping materials to all the rods.

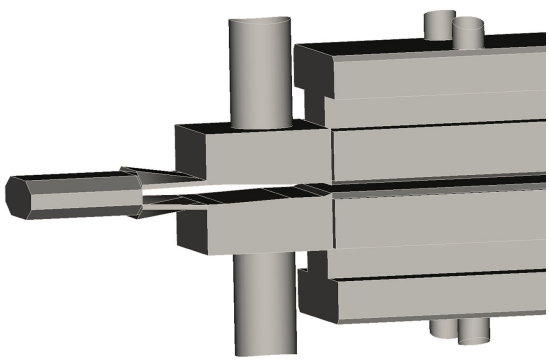

Figure 2: The simplified numerical simulation model with the vacuum chamber being hidden.

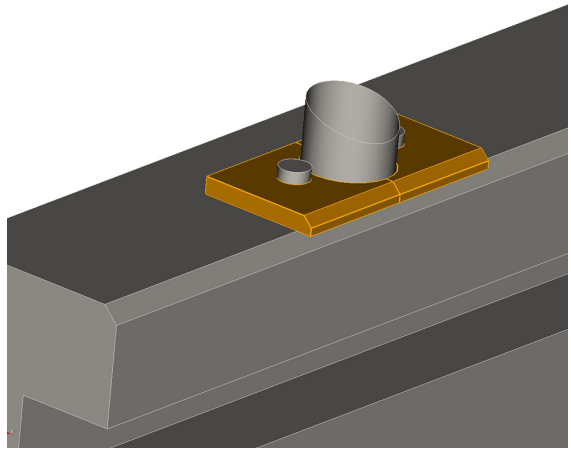

Figure 3: The numerical simulation model for a pair of ferrite dampers.

The final design of the dampers consists of 24 pairs of ferrite brackets with each pair attached around each rod. Each ferrite is mounted on the girder using a stainless steel bolt with sufficient pressure to ensure tight contact between the ferrite and the girder for efficient thermal conductance. The simulation model for a pair of the ferrite bracket is shown in Fig. 3, where the bolts are also included in the model. For the damping materials, we have chosen commercially available ferrites, TT2-111, which have been experimentally tested for damping the HOMs in LHC collimators [17–19].

DAMPER PERFORMANCE

The permittivity and permeability of ferrite materials are both complex, frequency dependent quantities that can be represented by $\mu_r = \mu' - i\mu''$ and $\epsilon_r = \epsilon' - i\epsilon''$. Because Omega3P only allows fixed material properties for each run, we split the simulation into 4 runs to solve for the RF modes in different ranges of frequencies and change the material properties in each run so that we can take into account the frequency dependent variation of the ferrite material [19].

ISBN: 978-3-95450-208-0 doi:10.18429/JACoW-IPAC2019-TUPRB101

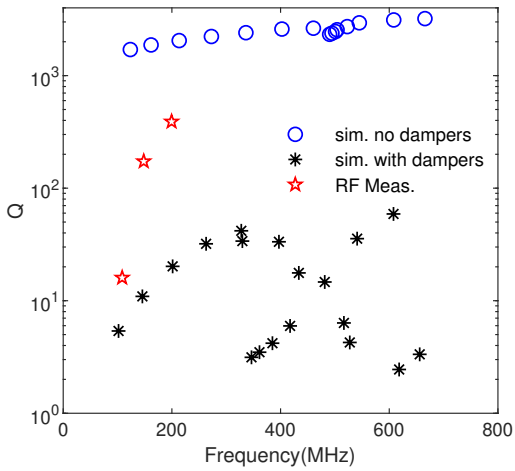

Figure 4: Simulation results of quality factors of the trapped RF modes in the IVU with and without ferrite dampers.

In Fig. 4, we plot the simulation results of the quality factors of the trapped RF modes up to 800 MHz for the IVU chamber before (blue circles) and after (black stars) adding the ferrite dampers. For comparison, the Q values of the three trapped modes measured in the cold RF measurements are also shown in the same plot (red pentagrams). As expected, after installing these ferrite dampers, the Q values for all modes drop significantly. Particularly, for the first three modes, the loaded Q drops by over two order of magnitude in simulations. With the dampers, the loaded Q of HOM mode #2 and #3 would have comparable values with the measured Q_L of HOM mode #1 from the RF cold test. Since HOM mode#1 didn't cause any beam instabilities in BL15 ID, these indicate that both modes would be sufficiently damped such that they would not cause any beam instabilities. One should note that the discrepancy between the Q's from RF test and simulation for the ID without ferrite dampers is due to the inexact modeling for both the surface material and ID structure.

In the new BL17 ID, the most recently ordered device for SPEAR3 with almost identical design to the BL15 ID,our design of ferrite dampers are successfully incorporated; therefore, this device can serve as the first test-bed for the performance of these dampers. Due to some technical constraints, only 22 pairs, instead of the intended 24 pairs of ferrite brackets, were eventually installed in the chamber.

The performance of the ferrite dampers is well illustrated in Fig. 5, where the measured loaded Q of BL17 ID at various gaps and that of BL15 ID (pentagrams) at 6.82mm are shown together for comparison. The values for the loaded Q of the first three modes for BL15 ID at 6.82mm gap are 16, 173, and 390 respectively. After adding the dampers in BL17 ID, at 6.79 mm gap, the loaded Q of these three modes are 14.3, 16.8, and 24.8, respectively. The modes are not only effective damped in order to prevent beam instabilities, the measurements also show good agreement with the

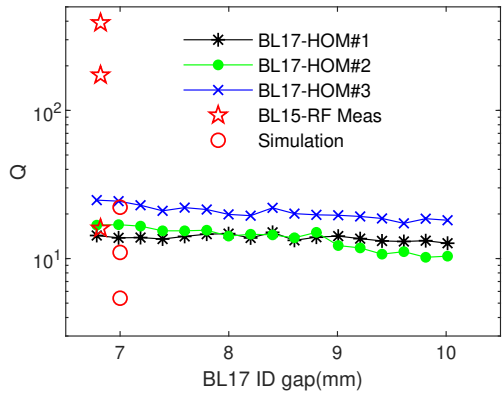

Figure 5: RF cold test results for BL17 ID with ferrite dampers:RF modes Q. vs ID magnet gap (bottom).

simulation results, shown as red circles in the plot, which predict the Q of HOM #3 to be 20.2. However, the simulation predicts much stronger damping effects for HOM #1 and #2. These differences have no impact in solving the problem of beam instabilities caused by these trapped RF modes.

CONCLUSION

In SPEAR3, we have developed an effective migration technique for the coupled-bunch instabilities caused by the IVU, nonetheless, more studies are required to fully understand the exact impedances effects from the IVU device. Such studies are beyond the operational requirement of SPEAR3, but are important for future diffraction limited storage ring facilities, for which, the impedance budgets are harder to meet due to small vacuum chambers. In order to explore the effects of the complex geometric features and material properties of the IVU device on the beam coupling impedances, extra efforts will be required to improve the numerical model for the simulations. Furthermore, it is desirable to directly measure the transverse coupling impedance of the IVU device using beam based technique or on bench low level RF techniques so that the results can be compared with numerical simulations for benchmark. All these studies will be beneficial to both the next generation SR facilities for high brightness operation and the IVU designers to minimize the impedance effects from the design phase.

ACKNOWLEDGEMENTS

We want to thanks J. Safranek, T. Rabedau, D. Teytleman, X. Huang, N. Kurita, V. Dolgashev, and A. Krasnykh for useful discussion, J. Vargas, B. Evanson, P. Velikov, G. Lanza, T. Dinan, and A. Haase for their technical supports in testing and measurements, andG. Rehm, S. Milward, J. Chavanne, E. Wallen, S. Santis, and R. Dowd for sharing with us their operating experiences with IVUs.

ISBN: 978-3-95450-208-0 doi:10.18429/JACoW-IPAC2019-TUPRB101

REFERENCES

[1] R. Dowd, M. Atkinson, M. J. Boland, G. S. Leblanc, Y.-R. E. Tan, and D. Teytelman, "Investigation of trapped resonant modes in insertion devices at the Australian Synchrotron," in *Proceedings of the 7th International Particle Accelerator Conference*, Busan, Korea: JACow, 2016, p. 1710.

[2] G. Rehm, "Measurement of rf resonances and measured impact on transverse multibunch instabilities from in-vacuum insertions devices," in *Proceedings of the 8th International Particle Accelerator Conference*, Copenhagen, Denmark: JACoW, 2017, p. 3188.

[3] R. Bartolini, R. Fielder, and G. Rehm, "Multi-bunch instabilities measurement and analysis at the Diamond Light Source," in *Proceedings of the 8th International Particle Accelerator Conference*, Copenhagen, Denmark: JACoW, 2017, p. 4485.

[4] K. Tian, J. Sebek, and J. L. Vargas, "Investigation of transverse beam instability induced by an in-vacuum undulator at SPEAR3," in *Proceedings of the 2016 International Beam Instrumentation Conference*, Barcelona, Spain: JACoW, 2016, p. 31.

[5] K. Tian, J. J. Sebek, A. D. Ringwall, and Z. Li, "Damping trapped modes in an in-vacuum undulator at a synchrotron radiation light source," *Phys. Rev. Accel. Beams*, vol. 22, p. 050 702, 2019.

[6] S. B. Cohn, "Properties of ridge wave guide," *Proceedings of the IRE*, vol. 35, p. 78, 1947.

[7] S. Hopfer, "The design of ridged waveguides," *IRE Trans. Microwave Theory Tech.*, vol. MTT-3, p. 20, 1955.

[8] S. Ramo, J. R. Whinnery, and T. V. Duzer, *Fields and Waves in Communication Electronics*. John Wiley & Sons, Inc., 1994.

[9] A. Chao, *Physics of Collective Instabilities in High Energy Accelerators*. John Wiley & Sons, Inc., 1993.

[10] D. Teytelman, "Overview of system specifications for bunch by bunch feedback systems," in *Proceedings of the 2011 Particle Accelerator Conference*, New York: IEEE, 2011, p. 1475.

[11] D. Teytelman, "Optimization of bunch-to-bunch isolation in instability feedback systems," in *Proceedings of the 2013 International Beam Instrumentation Conference*, Oxford, UK: JACoW, 2016, p. 116.

[12] M. Lonza, "Multi-bunch feedback systems," in *2007 CERN Accelerator School*, Sigtuna, Sweden, 2007. http://cds.cern.ch/record/1213287/files/p467.pdf.

[13] NERSC website: http://www.nersc.gov/

[14] CUIBIT website: https://cubit.sandia.gov/

[15] ParaView website: https://www.paraview.org/

[16] R. Reiser *et al.*, "The flexible taper transitions for an in-vacuum undulator," in *Proceedings of MEDSI'02*, 2008, p. 323.

[17] N. Biancacci *et al.*, "Impedance simulations and measurements on the LHC collimators with embedded beam position monitors," *Phys. Rev. Accel. Beams*, vol. 20, p. 011 003, 2017.

[18] A. Bertarelli and M. Garlaschè, "Design guidelines for ferrite absorbers submitted to rf-induced heating," in *Proceedings of the 4th International Particle Accelerator Conference*, Shanghai, China: JACow, 2013, p. 3394.

[19] TT2-111R Data Sheet, courtesy of Trans Tech, Adamstown, Maryland.